

Refined CT-Based Proxy for Foraminiferal Diagenesis Shows Evidence for Shallow Dissolution in North Atlantic Sediment Cores.

5 Weiss, Thomas L.^{1,2,3}; Fabbrini, Alessio¹; McManus, Jerry F.^{4,5}; de la Vega, Elwyn¹; Krishnakumar, Hridya¹; Morley, Audrey^{1,2}

¹University of Galway, School of Geography, Archaeology, and Irish Studies, Galway, Ireland

²iCRAG—Irish Centre for Research in Applied Geosciences, Belfield, Dublin 4, Ireland

³Georgia Institute of Technology, Atlanta, Georgia

10 ⁴Lamont-Doherty Earth Observatory, Columbia University, Palisades, NY 10964, USA

⁵Department of Earth and Environmental Sciences, Columbia University, New York, NY 10027, USA

Corresponding authors: Thomas Weiss (tweiss9@gatech.edu) and Audrey Morley (audrey.morley@universityofgalway.ie)

15 Supplementary Material

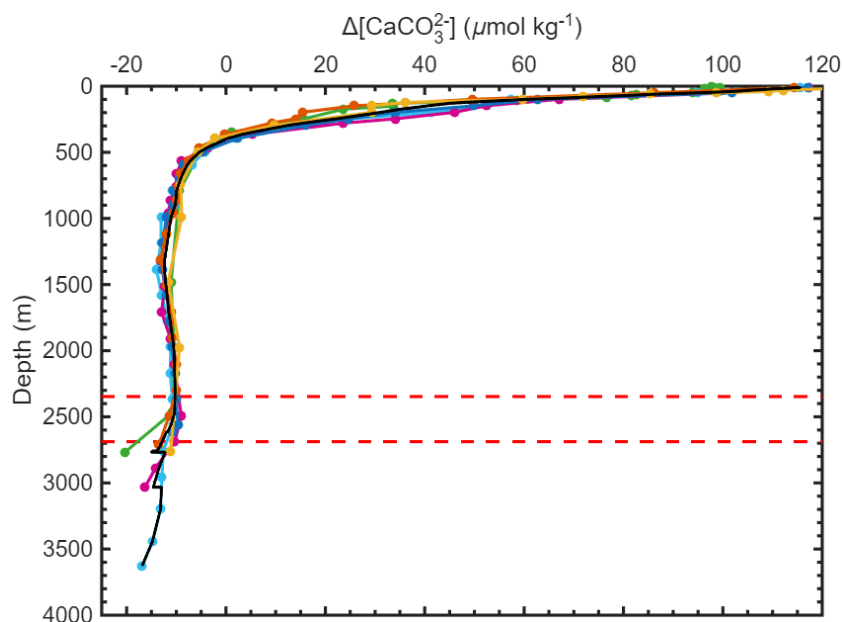
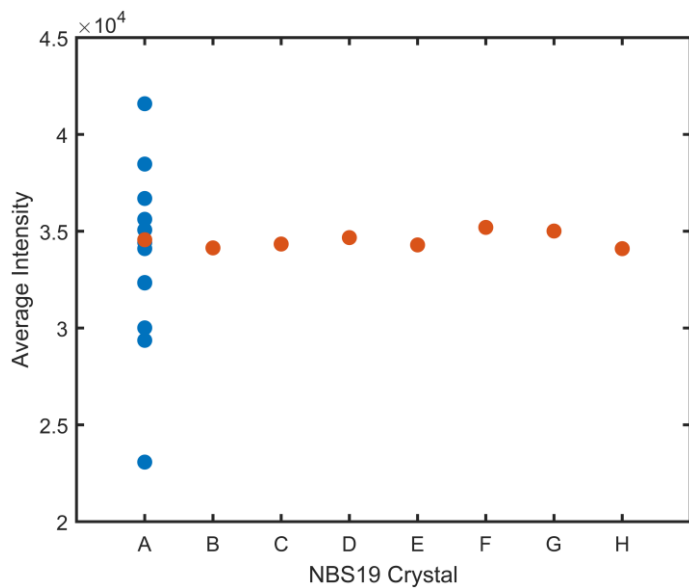
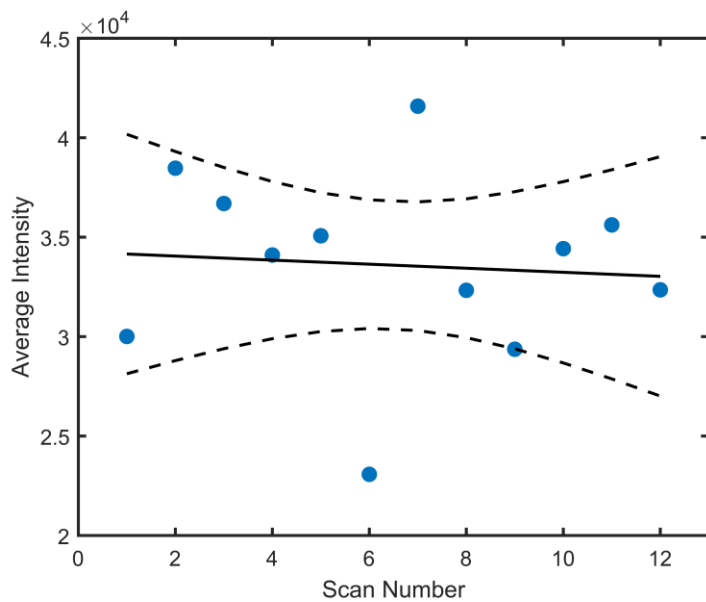


Figure S1— $\Delta[\text{CO}_3^{2-}]$ profiles calculated from DIC, alkalinity, temperature, and salinity from the five GLODAP stations nearest to the AT26-19 stations. The black line is the average of the five profiles interpolated to 1 m resolution. Red dashed lines are the depths of the two AT26-19 stations used for this study.



20

Figure S2— Comparison of average intensities between eight different NBS19 crystals analyzed in a single scan (orange) and the average intensity of a single NBS19 crystal over 12 scans using the same settings as this study (blue). Low variability between different crystals of the same scan demonstrates NBS19 crystals have a consistent density.



25

Figure S3— Long term average intensity for a single NBS19 crystal (blue) scanned using the same settings as this study and linear regression (solid black line) and 95% confidence interval (dashed black lines). The linear regression has $r^2=0.006$ and the slope has a p-value of 0.81, indicating no significant change in intensity over time and that repeated scans are not reducing the density of the standard.

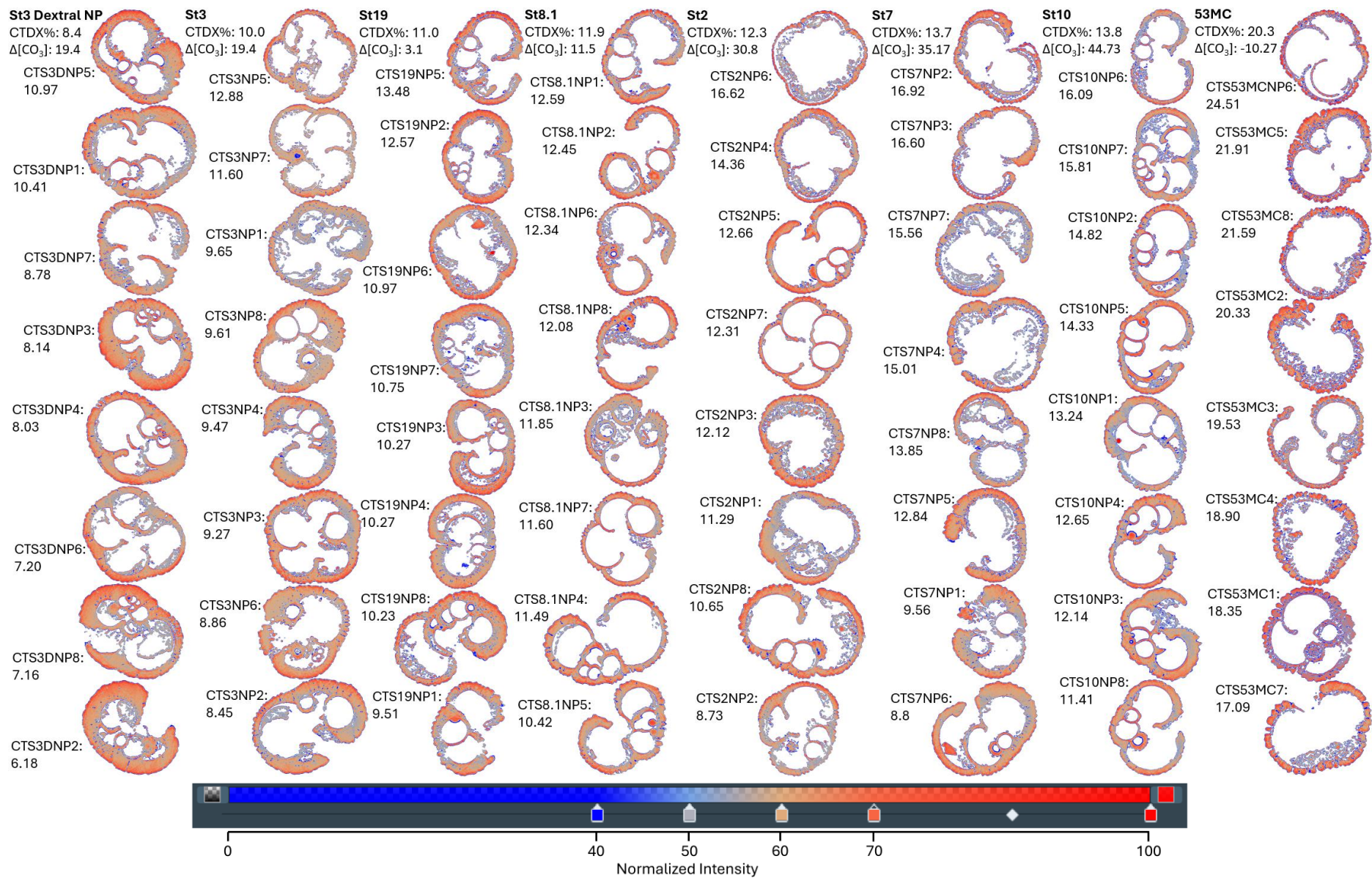


Figure S4—Core top *N. pachyderma* cross-section density maps. Each column is one station with nCTDX% increasing upward. Average station nCTDX% increases moving right.

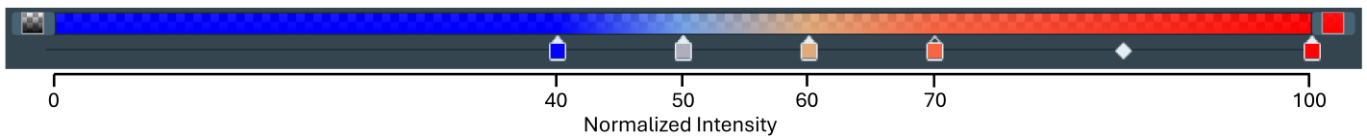
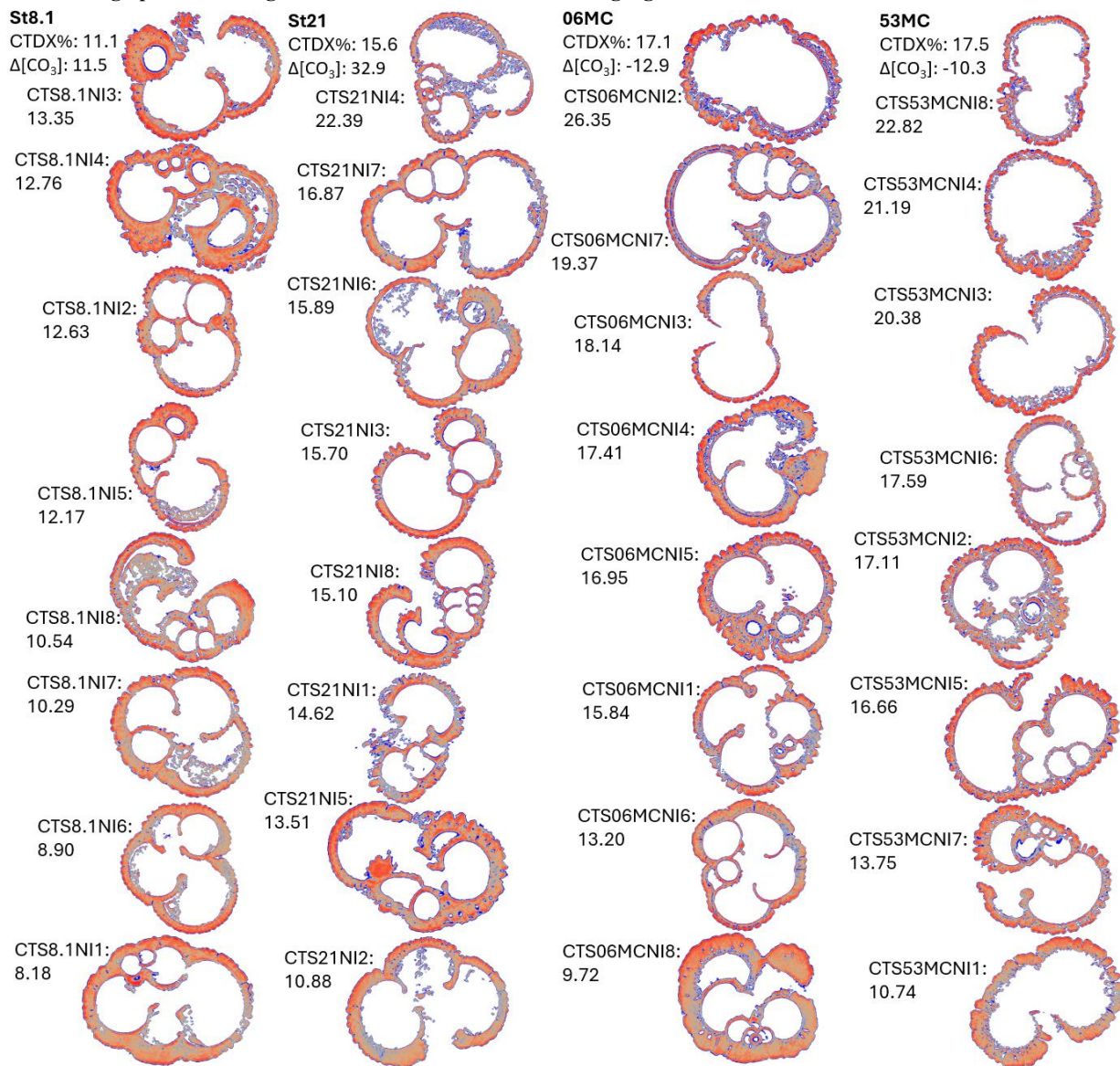


Figure S5—Core top *N. incompta* cross-sectional density maps. Each column is one station with nCTDX% increasing upward. Average station nCTDX% increases moving right.

Figure S6— Downcore *N. pachyderma* cross-section density maps. Each column is one station with nCTDX% increasing upward. Average station nCTDX% increases moving right.

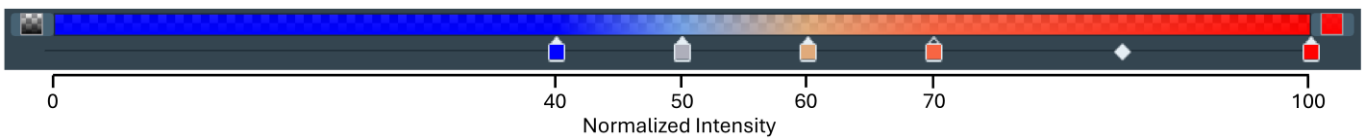
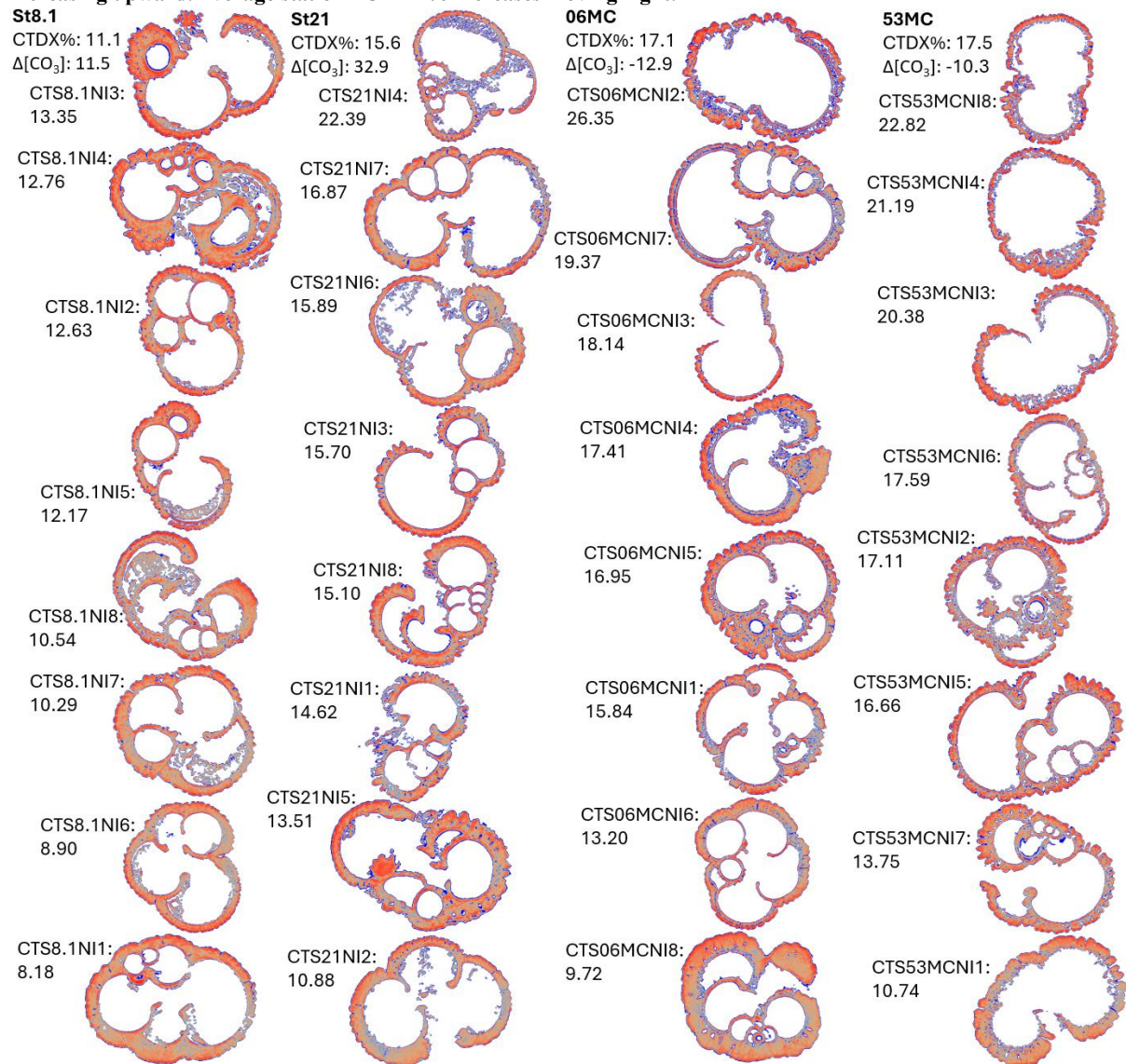


Figure S7— Downcore *N. incompta* cross-section density maps. Each column is one station with nCTDX% increasing upward. Average station nCTDX% increases moving right.

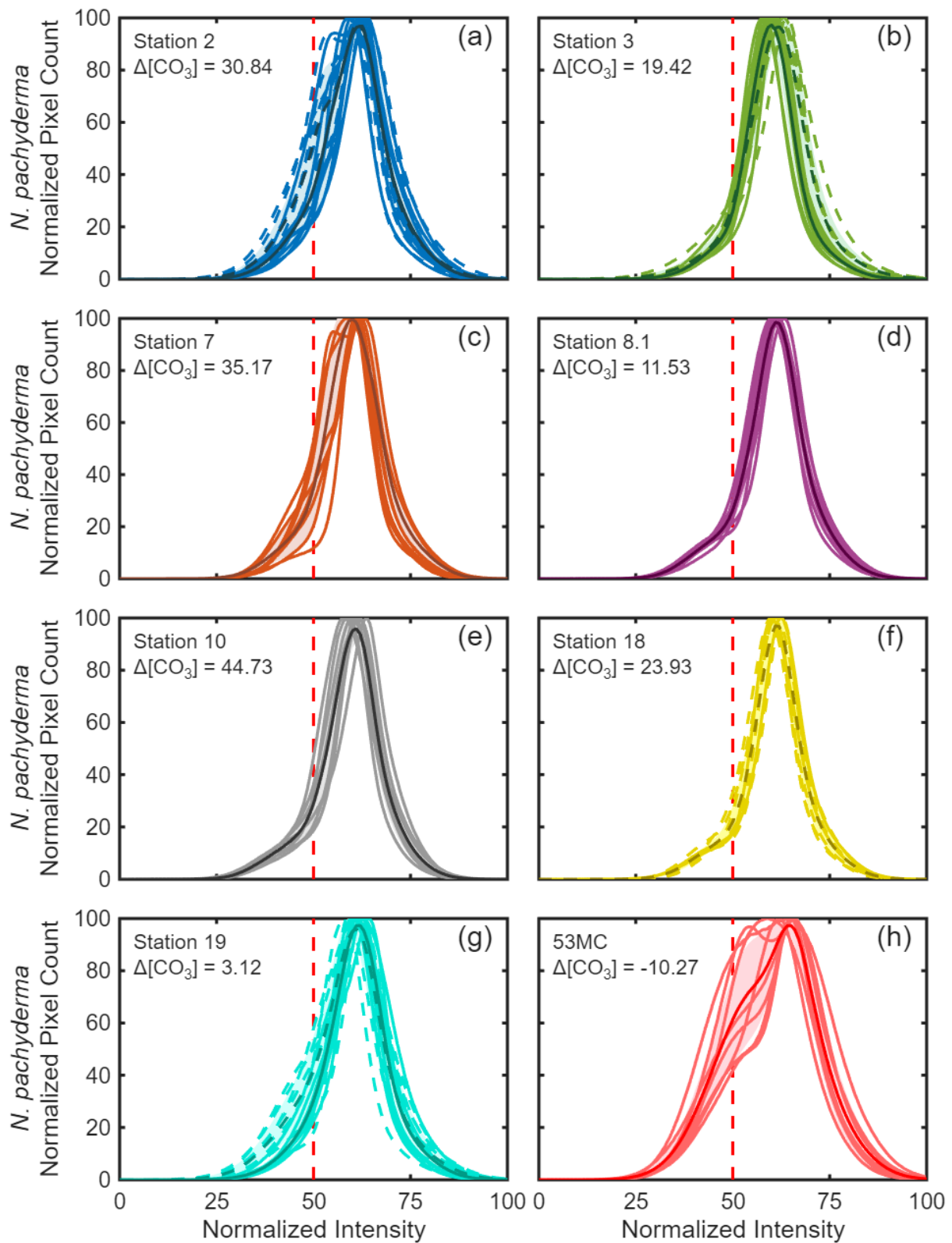


Figure S8—(a-i) Normalized pixel counts at each normalized μCT scan intensity for each individual *N. pachyderma* specimen for each core top (solid lines) and downcore (dashed lines) sample (light colors). Dark colors and light shading represent the average and standard deviation normalized pixel count as plotted in Fig. 4.

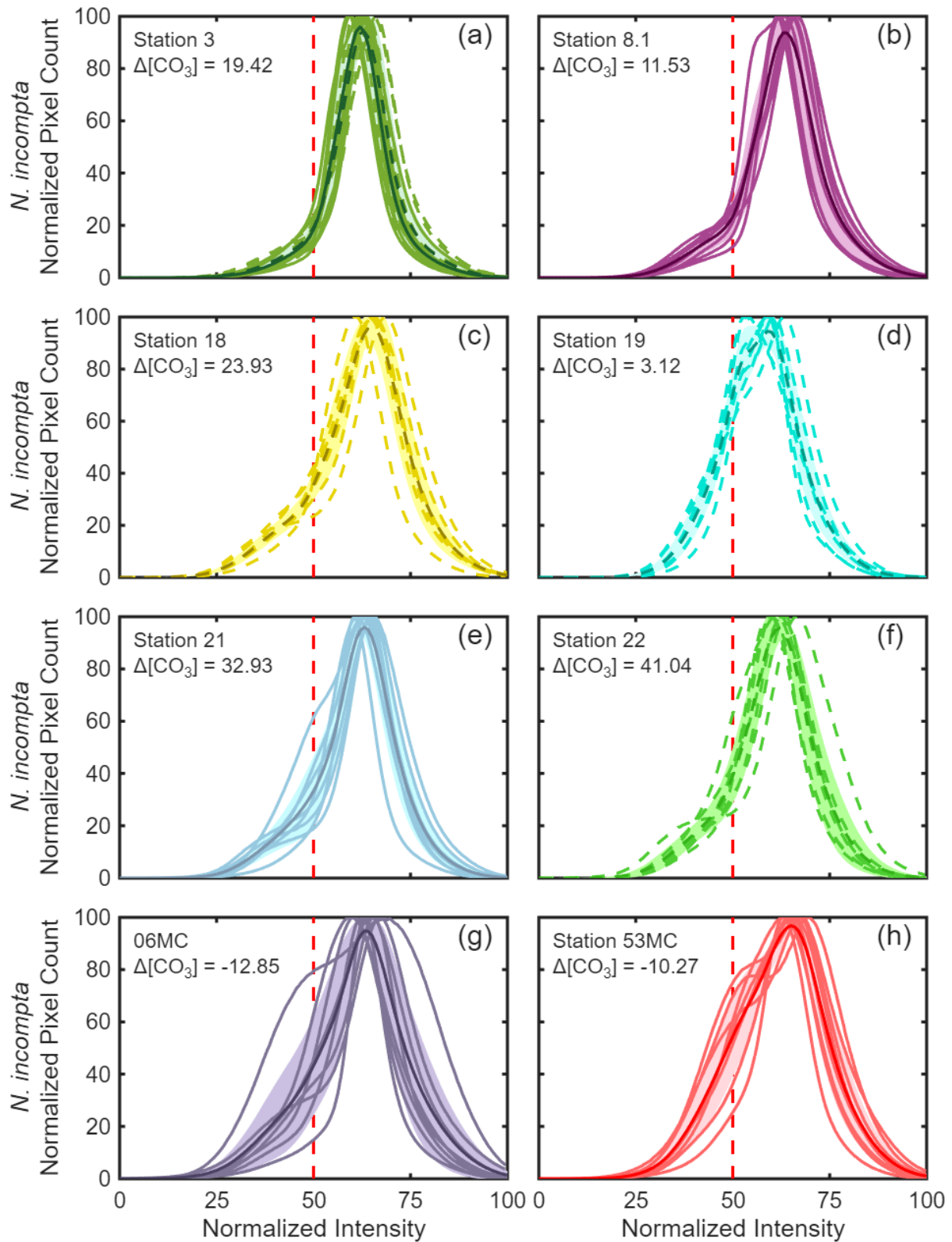


Figure S9—(a-h) Normalized pixel counts at each normalized μCT scan intensity for each individual *N. incompta* specimen for each core top (solid lines) and downcore (dashed lines) sample (light colors). Dark colors and light shading represent the average and standard deviation normalized pixel count as plotted in Fig. 4. Station 3 core top and downcore specimens are dextrally coiling *N. pachyderma*.

Adjacent Stations from This Study	Core	Latitude (°N)	Longitude (°E)	Core Depth (cm)	Calibrated Age (ka)	Holocene Sedimentation Rate (cm/ka)	Reference	
2 and 3	PS1894-7	75.8	-8.2	0.5	3.81		Nørgaard-Pedersen et al., 2003	
				9.5	6.17			
	PS1906-1	76.9	-2.2	4.5	4.50			Nørgaard-Pedersen et al., 2003
	PS1535-5	78.8	1.8	0	0.28			Nørgaard-Pedersen et al., 2003
				7.5	4.97			
18 and 19	D298-P2	57.6	-48.5			32	Davies et al., 2021	
	D298-P3	58.2	-48.4			23	Davies et al., 2021	
	TTR13AT-450G	58.0	-45.8			0.4	Davies et al., 2021	
22	GIK23415-9	53.2	-19.1	2.5	1.88		Jung, 2004	

Table S1—Calibrated ages and estimated sedimentation rates for cores collected near cores from this study with downcore samples.

References

Davies, S., Stow, D., and Nicholson, U.: Late glacial to Holocene sedimentary facies of the Eirik Drift, southern Greenland margin: Spatial and temporal variability and paleoceanographic implications, *Marine Geology*, 440, 106568, <https://doi.org/10.1016/j.margeo.2021.106568>, 2021.

Jung, S. J. A.: Radiocarbon age determinations on sediment core GIK23415-9., <https://doi.org/10.1594/PANGAEA.186490>, 2004.

Nørgaard-Pedersen, N., Spielhagen, R. F., Erlenkeuser, H., Grootes, P., Heinemeier, J., and Knies, J.: Arctic Ocean during the Last Glacial Maximum: Atlantic and polar domains of surface water mass distribution and ice cover, *Paleoceanography and Paleoclimatology*, 18, <https://doi.org/10.1029/2002PA000781>, 2003.